


Dynamic spin polarization in organic semiconductors with intermolecular exchange interactionA. V. Shumilin *Ioffe Institute, Russian Academy of Sciences, 194021 St. Petersburg, Russia*

(Received 13 December 2021; revised 7 March 2022; accepted 7 March 2022; published 24 March 2022)

It is shown that in organic semiconductors where organic magnetoresistance (OMAR) is observed, the exchange interaction between electrons and holes localized at different molecules leads to dynamic spin polarization in the direction of the applied magnetic field. The polarization appears even at room temperature due to the nonequilibrium conditions. The strong spin polarization requires the exchange energy to be comparable to the Zeeman energy in the external field and to be larger than or comparable to the energy of hyperfine interaction of electron and nuclear spins. The exchange interaction also modifies the shape of OMAR.

DOI: [10.1103/PhysRevB.105.104206](https://doi.org/10.1103/PhysRevB.105.104206)**I. INTRODUCTION**

Organic semiconductors represent a novel class of materials that attracts significant interest nowadays. They are widely applied as light-emitting diodes [1,2]. Other possible applications are organic solar cells [3–5] and organic transistors [6,7]. These semiconductors are promising materials for spintronics due to the long spin relaxation times and spin diffusion lengths that can reach dozens of nanometers [8–10]. In addition, the spin transport in organic semiconductors is related to several intriguing phenomena that are not always well understood.

The organic spin valves are unexpectedly easy to produce [11]. The conductivity of organic semiconductors is usually much smaller than that of magnetic contacts. It should exclude spin-valve magnetoresistance due to the spin injection [12]. The thickness of the devices often exceeds 100 nm and does not allow the tunneling through the organic layer [13]. However, spin-valve magnetoresistance of the order of 10% is measured in numerous experiments. Although an explanation related to exchange interaction between carriers localized on different molecules was provided by Yu [14], the reason for strong spin-valve magnetoresistance in organic devices is still under discussion. While some groups report spin injection from magnetic contacts to organic semiconductors, other groups consider this injection to be impossible [15]. In this situation the nontransport detection of spin polarization in organics can be important. Such a detection was made with muon spin rotation and showed the existence of spin polarization in a working organic spin-valve device [10].

Another interesting property of spin transport in organic semiconductors is the so-called organic magnetoresistance (OMAR) [16,17]. This is the strong magnetoresistance observed in magnetic fields of 10–100 mT both at low and room temperature. In contrast to the strong organic spin-valve effect this phenomenon is generally understood. Several mechanisms of OMAR were proposed [18–20]. The magnetoresistance appears because out of equilibrium the interaction between electrons and holes leads to correlations of electron and hole spins. These correlations can affect transport

in organic semiconductors. Different mechanisms of OMAR are related to different nonequilibrium processes including exciton generation [18] and electric current combined with the possibility of double occupation of molecular orbitals [19]. The applied magnetic field suppresses the relaxation of spin correlations that is caused by the hyperfine interaction of electron and nuclear spins [21]. This modifies the statistics of spin correlations and leads to magnetoresistance.

The general understanding of OMAR requires only the interplay of nonequilibrium carrier statistics and the hyperfine interaction of electron and nuclear spins. However, in some cases the exchange interaction between electrons localized on neighbor molecules is invoked to describe the properties of OMAR in particular materials [22,23].

In this paper it is shown that the interplay of the exchange interaction, hyperfine interaction of electron and nuclear spins, and nonequilibrium phenomena in organic semiconductors leads to the polarization of electron spins. The polarization occurs when the Zeeman energy is comparable to the energies of hyperfine and exchange interactions. The temperature is considered to be much larger than all these energies. To the best of the author's knowledge, this phenomenon has never been discussed in organic semiconductors. However, a similar effect was recently observed in inorganic semiconductor quantum dots [24,25], where the spin polarization can reach dozens of percents, and theoretically predicted in transition-metal dichalcogenides bilayers [26]. The effect was called the dynamic spin polarization, in contrast to the thermal spin polarization that requires the Zeeman energy to be larger than or comparable to the temperature.

The paper is organized as follows. In Sec. II the model of organic semiconductor is introduced. This model includes the mechanisms of OMAR that are also responsible for the dynamic spin polarization when the exchange interaction is taken into account. In Sec. III the master equations are derived that describe the spin dynamics due to hopping, hyperfine interaction, and exchange interaction. In Sec. IV the effect of the exchange interaction on conductivity and exciton generation rate is described. In Sec. V the dynamic spin polarization is

obtained by the numeric solution of equations derived before. In Sec. VI the specific “resonance” case is treated analytically. In Sec. VII the general discussion and conclusion of the results of this paper are given.

II. MODEL

Organic semiconductors are amorphous materials composed of single molecules or short polymers. The transport in these materials is due to the hopping of electron and hole polarons over molecular orbitals [27,28]. Typically, organic semiconductors are strongly disordered due to the distribution of the energies of molecular orbitals with the width exceeding 0.1 eV [29,30], which is large in comparison to the room temperature. Also the overlap integrals between neighbor molecules differ in orders of magnitude [31] enhancing the disorder in organic semiconductors.

The following model of an organic semiconductor is adopted in this paper. Two molecular orbitals in each molecule are considered: the highest occupied molecular orbital (HOMO) and the lowest unoccupied molecular orbital (LUMO). The charge transport is due to the hopping of electron polarons over the LUMO, due to the hopping of hole polarons over the HOMO, and in the case of bipolar devices due to the generation of excitons from electron-hole pairs and their subsequent recombination.

The strong disorder localizes the current in a rather sparse percolation cluster, and the resistivity is controlled by rare bottlenecks in this cluster [32,33]. These bottlenecks are pairs of molecular orbitals with a relatively slow hopping rate between them. In the case of bipolar devices the bottlenecks can also be pairs of a HOMO and a LUMO where electrons and holes recombine or form excitons.

The dynamic spin polarization is related to the same phenomena that lead to OMAR. The two most known mechanisms of OMAR are the electron-hole (or exciton) mechanism and the bipolaron mechanism. The electron-hole mechanism exists only in bipolar devices and is related to the different rates of singlet and triplet exciton generation or to the different rates of recombination of electrons and holes composing singlet or triplet exciplets [18]. The bipolaron mechanism can also exist in unipolar devices but requires the possibility of double occupation of molecular orbitals. It is assumed that double occupation is possible only for electrons or holes in the spin-singlet state [19]. To describe OMAR and dynamic polarization, the theory of hopping transport that includes correlation of spins and occupation numbers should be used. Such a theory developed in Refs. [34–37] is applied in this paper.

Both electron-hole and bipolaron mechanisms of OMAR are considered, and the unified description for both the mechanisms is given when possible.

In the case of the electron-hole mechanism the bottlenecks that control conductivity are considered to be pairs of trapping sites for an electron and a hole (see Fig. 1). In such a pair the singlet exciton can be composed with the rate γ_s , and the triplet one can be composed with the rate γ_t . After its generation the strong exchange interaction prevents the exciton from changing its type. The singlet excitons then recombine radiatively. Triplet excitons recombine either due

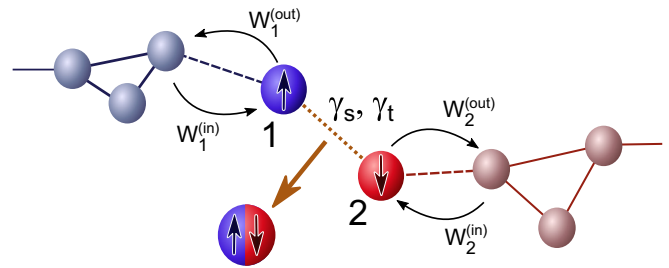


FIG. 1. Electron-hole mechanism of OMAR. LUMO of molecules including the electron trapping site 1 are shown in blue. HOMO including the hole trapping site 2 are shown in red. Black arrows correspond to the rates of hopping to or from trapping sites. γ_s and γ_t are the rates of singlet and triplet exciton formation. The excitons recombine either radiatively or nonradiatively but never dissociate.

to phosphorescence [38,39] or due to nonradiative processes. In the studied model the existing excitons do not affect the charge transport or formation of new excitons. The current J through the bottleneck is proportional to the rate of exciton generation

$$J = e\gamma_s \frac{\overline{n_1 n_2} - 4s_1^{(\alpha)} s_2^{(\alpha)}}{4} + e\gamma_t \frac{3\overline{n_1 n_2} + 4s_1^{(\alpha)} s_2^{(\alpha)}}{4}. \quad (1)$$

Here, $\overline{n_1 n_2}$ is the probability of the joint occupation of LUMO site 1 with an electron and HOMO site 2 with a hole. $s_1^{(\alpha)} s_2^{(\beta)}$ is the averaged product of spin polarization on site 1 along Cartesian direction α and spin polarization on site 2 along the direction β . The sum over the repeating index α is assumed in Eq. (1).

Without average spin polarizations, $s_1^{(\alpha)} s_2^{(\beta)}$ describe the correlations of spin directions. They can be expressed in terms of spin density matrix ρ_s as follows:

$$\overline{s_1^{(\alpha)} s_2^{(\beta)}} = \frac{1}{4} \text{Tr}[\sigma_1^{(\alpha)} \sigma_2^{(\beta)} \rho_s]. \quad (2)$$

Here, $\sigma_1^{(\alpha)}$ is the Pauli matrix related to direction α and acting on the spin of trapping site 1. $\sigma_2^{(\beta)}$ is a similar matrix for site 2.

$\overline{s_1^{(\alpha)} s_2^{(\beta)}}$ are equal to zero in equilibrium because the temperature is large and ρ_s is proportional to the identity matrix. It will be shown in Sec. III that $\overline{s_1^{(\alpha)} s_2^{(\beta)}}$ is proportional to J and the current can be expressed as follows:

$$J = e\gamma_{eh}(B)\overline{n_1 n_2}. \quad (3)$$

Here, $\gamma_{eh}(B)$ is the effective exciton generation rate that depends on the applied magnetic field B .

Sites 1 and 2 are connected to other parts of the percolation cluster. The electron can be trapped on molecule 1 with the rate $W_1^{(in)}$ and be released with rate $W_1^{(out)}$. $W_2^{(in)}$ and $W_2^{(out)}$ are similar rates for a hole to be trapped on site 2 and leave it, respectively (see Fig. 1 for the directions of hops corresponding to these rates). $W_{1,2}^{(in)}$ and $W_{1,2}^{(out)}$ are considered not to depend on the magnetic field. This allows one to express the magnetoresistance as a function of γ_{eh} . The corresponding derivations are provided in Appendix A. When the magnetoresistance is relatively small, it can be expressed as

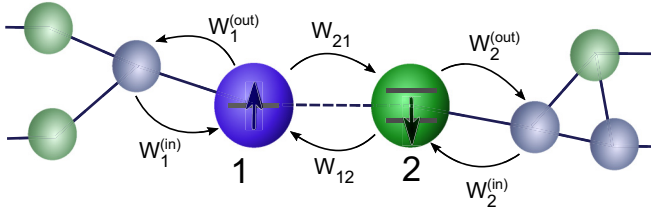


FIG. 2. Bipolaron mechanism of OMAR. A-type LUMOs are shown with blue color, and B-type LUMOs are shown with green color. Black arrows correspond to the rates of hopping to or from the bottleneck.

follows:

$$\frac{R(B) - R(0)}{R(0)} = - \left\langle C_{eh} \frac{\gamma_{eh}(B) - \gamma_{eh}(0)}{\gamma_{eh}(0)} \right\rangle. \quad (4)$$

Here, $R(B)$ is the sample resistance, and $\langle \dots \rangle$ describes the averaging over bottlenecks where exciton generation occurs. C_{eh} is the constant that is derived in Appendix A.

The bipolaron mechanism of OMAR exists both in bipolar and unipolar devices. In this paper it is discussed for unipolar devices with conductivity provided by electrons. It is assumed that the LUMO can be double occupied by two electrons in the spin-singlet state. The energy of double occupation is larger than the energy of single occupation by the Hubbard energy $E_H \gg T$. In this case all the molecular orbitals participating in hopping transport can be divided into the two types. The A-type orbitals can be unoccupied or single occupied but are never double occupied due to the large Hubbard energy. The B-type orbitals have very low energy of single occupation and therefore are always occupied by at least one (resident) electron. Sometimes they are double occupied by an electron pair in the spin-singlet state. Note that both types of orbitals are LUMOs.

The bottlenecks in the unipolar transport are the pairs of orbitals with the slowest hopping rates that are included into the percolation cluster. Only the pairs of LUMOs with different types are important for the bipolaron mechanism of OMAR. Such a pair is shown in Fig. 2. I call the LUMO in the bottleneck the hopping sites 1 and 2 with analogy to the trapping sites in the electron-hole mechanism. Site 1 corresponds to the A-type molecular orbital, and site 2 has type B for definiteness.

The current in the bottleneck can be expressed as follows:

$$J = \frac{eW_{21}}{2} (\bar{n}_1 - 4\overline{s_A^{(\alpha)} s_B^{(\alpha)}} - \bar{n}_1 \bar{n}_2) - 2eW_{12} \overline{n_2(1 - n_1)}. \quad (5)$$

Here, $\bar{n}_1 \bar{n}_2$ is the probability of joint occupation. W_{12} and W_{21} are the rates of hops inside the bottleneck as shown in Fig. 2. Similarly to the electron-hole mechanism, it will be shown that $\overline{s_1^{(\alpha)} s_2^{(\alpha)}}$ is proportional to the current J . This allows one to express J as follows:

$$J = \kappa_{bp}(B) J_0, \quad (6)$$

$$J_0 = \frac{eW_{21}}{2} \overline{n_1(1 - n_2)} - 2eW_{12} \overline{n_2(1 - n_1)}. \quad (7)$$

Here, $\kappa_{bp}(B)$ is the probability of the electron to be transferred through the critical pair. It depends on the applied magnetic

field leading to OMAR. When $|\kappa_{bp}(B) - \kappa_{bp}(0)| \ll \kappa_{bp}(0)$, the magnetoresistance can be expressed as follows:

$$\frac{R(B) - R(0)}{R(0)} = - \left\langle \frac{\kappa_{bp}(B) - \kappa_{bp}(0)}{\kappa_{bp}(0)} \right\rangle. \quad (8)$$

III. SPIN DYNAMICS

In this section the dynamic of spin and spin correlations in the bottlenecks is described. The temperature is considered to be large compared with the Zeeman energy of the electron spins, the energy of the hyperfine interaction, and the exchange energy; therefore in equilibrium there is no spin polarization or correlations of spin directions. The spin correlations appear in the nonequilibrium processes. For example, if OMAR is controlled by the electron-hole mechanism and the singlet exciton formation is more probable than the formation of the triplet exciton, the triplet state of the electron-hole pair in the bottleneck would be more probable than the singlet state. I assume that when electrons and holes leave the bottleneck sites and go to the percolation cluster, they mix with other electrons and holes and the spin correlation is forgotten. This leads to an effective spin relaxation. Finally, the spin correlations have coherent dynamics in the bottleneck due to hyperfine interaction with atomic nuclei and exchange interaction.

The kinetics of spin correlations can be expressed as follows:

$$\frac{ds_1^{(\alpha)} s_2^{(\beta)}}{dt} = \frac{i}{\hbar} [H, s_1^{(\alpha)} s_2^{(\beta)}] + G\delta_{\alpha\beta} - R_{\alpha\beta;\alpha'\beta'} \overline{s_1^{(\alpha')} s_2^{(\beta')}}. \quad (9)$$

Here, the first term on the right-hand side describes the coherent spin dynamics due to hyperfine interaction with atomic nuclei, the external magnetic field, and the exchange interaction. H is the Hamiltonian that includes all these energies. $G\delta_{\alpha\beta}$ stands for the generation of spin correlations due to the nonequilibrium processes. $R_{\alpha\beta;\alpha'\beta'}$ describes the relaxation of spin correlations due to electron transfer between the bottleneck and other parts of the percolation cluster. $R_{\alpha\beta;\alpha'\beta'}$ also includes some contribution to the relaxation of spin correlations due to the incoherent processes inside the bottleneck.

In the bipolaron mechanism the generation of spin correlations is proportional to the current

$$G = \frac{J}{4e}, \quad (10)$$

and the relaxation is described with the expression

$$R_{\alpha\beta;\alpha'\beta'} = (W_1^{(out)} + W_2^{(in)}) \delta_{\alpha\alpha'} \delta_{\beta\beta'} + \frac{W_{21}}{2} (\delta_{\alpha\alpha'} \delta_{\beta\beta'} - \delta_{\alpha\beta'} \delta_{\beta\alpha'}). \quad (11)$$

This expression shows that spin correlation is forgotten when the electron leaves the A-type site 1 and goes to the percolation cluster. The existence of the correlation assumes that the B-type site 2 is single occupied. It cannot lose its last electron. However, the correlation is forgotten when the second electron comes to site 2 from the percolation cluster while the site 1 is occupied. The hops from site 1 to site 2 are possible only in the singlet state of the spins. Even without net current this leads to the relaxation of the coherent combination of singlet

and triplet states [37]. This is shown by the second term on the right-hand side of Eq. (11).

In the electron-hole mechanism of OMAR the spin correlations appear due to the different rates of singlet and triplet exciton formation

$$G = (\gamma_s - \gamma_t) \frac{\overline{n_1 n_2} - 4 \overline{s_1^{(\gamma)} s_2^{(\gamma)}}}{16}. \quad (12)$$

Note that the probability of exciton decomposition is neglected and therefore the formation of the exciton is possible only out of equilibrium. The relaxation of correlations for the electron-hole mechanism of OMAR can be described as follows:

$$\begin{aligned} R_{\alpha\beta;\alpha'\beta'} &= (W_1^{(\text{out})} + W_2^{(\text{out})} + \gamma_t) \delta_{\alpha\alpha'} \delta_{\beta\beta'} \\ &+ \gamma_s (\delta_{\alpha\alpha'} \delta_{\beta\beta'} - \delta_{\alpha\beta'} \delta_{\beta\alpha'}). \end{aligned} \quad (13)$$

This expression shows that the correlation is forgotten when the electron leaves site 1 or the hole leaves site 2 and goes to the percolation cluster. It is also transferred to the exciton in the process of triplet exciton formation. The singlet exciton formation is similar to the hop from the A-type site to the B-type site in the bipolaron mechanism and leads to the relaxation of the coherent combinations of singlet and triplet states.

The Hamiltonian H can be expressed with the same equation for both the OMAR mechanisms.

$$H = H_B + E_{ex} \mathbf{s}_1 \mathbf{s}_2. \quad (14)$$

Here, E_{ex} is the energy of exchange interaction of electron (or hole) spins on sites 1 and 2. H_B describes the spin interaction with external magnetic field and atomic nuclei

$$H_B = \mu_b g (\mathbf{B} + \mathbf{B}_{hf}^{(1)}) \mathbf{s}_1 + \mu_b g (\mathbf{B} + \mathbf{B}_{hf}^{(2)}) \mathbf{s}_2. \quad (15)$$

Here, \mathbf{B} is the external magnetic field. $\mathbf{B}_{hf}^{(1)}$ and $\mathbf{B}_{hf}^{(2)}$ are the so-called hyperfine fields that describe hyperfine interaction with atomic nuclei on sites 1 and 2, respectively. It is presumed that on different sites the carrier spins interact with different nuclei; therefore $\mathbf{B}_{hf}^{(1)}$ and $\mathbf{B}_{hf}^{(2)}$ are independent. The distribution density of hyperfine fields is

$$\mathcal{F}(\mathbf{B}_{hf}^{(1,2)}) = \frac{1}{(\sqrt{2\pi} \Delta_{hf})^3} \exp\left(-\frac{|\mathbf{B}_{hf}^{(1,2)}|^2}{2\Delta_{hf}^2}\right). \quad (16)$$

Here, $\Delta_{hf} \sim 10$ mT is the typical hyperfine field. Equation (16) describes the vector normal distribution, i.e., it is the product of three normal distribution densities of Cartesian components of $\mathbf{B}_{hf}^{(1,2)}$. The description of hyperfine interaction with static hyperfine field corresponds to the limit of many nuclear spins interacting with a single electron spin.

The interaction with external and hyperfine fields leads to precession of electron and hole spins with frequencies $\Omega_{1,2} = \mu_b g (\mathbf{B} + \mathbf{B}_{hf}^{(1,2)}) / \hbar$ related to sites 1 and 2

$$\frac{i}{\hbar} [H_B, s_1^{(\alpha)} s_2^{(\beta)}] = \epsilon_{\alpha\gamma\alpha'} \Omega_1^{(\gamma)} \overline{s_1^{(\alpha')} s_2^{(\beta)}} + \epsilon_{\beta\gamma\beta'} \Omega_2^{(\gamma)} \overline{s_1^{(\alpha)} s_2^{(\beta')}}. \quad (17)$$

The spin dynamics due to the exchange interaction can be described with the expression

$$\frac{i}{\hbar} E_{ex} [\mathbf{s}_1 \mathbf{s}_2, s_1^{(\alpha)} s_2^{(\beta)}] = \frac{1}{4} \frac{E_{ex}}{\hbar} \epsilon_{\alpha\beta\gamma} (\overline{s_1^{(\gamma)} s_2^{(0)}} - \overline{s_1^{(0)} s_2^{(\gamma)}}). \quad (18)$$

Here, $\overline{s_1^{(0)} s_2^{(\gamma)}}$ describes the polarization of site 2 in the direction γ while site 1 is single occupied.

$$\overline{s_1^{(0)} s_2^{(\gamma)}} = \frac{1}{2} \text{Tr}[\sigma_1^{(0)} \sigma_2^{(\gamma)} \rho_s], \quad (19)$$

which is similar to Eq. (2). $\sigma_1^{(0)}$ is the unit matrix that acts on single-occupied states of site 1. Therefore $s_1^{(0)}$ and $s_2^{(0)}$ are the operators of single occupation of sites 1 and 2, respectively.

For the electron-hole mechanism or for A-type sites in the bipolaron mechanism the ‘‘single occupation’’ and ‘‘occupation’’ are the same, and $s_{1,2}^{(0)} = n_{1,2}$. In the considered model of the bipolaron mechanism, site 2 is a B-type site, and in this case $s_2^{(0)} = 1 - n_2$ because it is single occupied when the second electron is absent. In what follows the notation $s_{1,2}^{(0)}$ is used when single occupation is important for spin degrees of freedom, and $n_{1,2}$ is used for the description of current.

It is often assumed that due to the time-reversal symmetry the statistics of spins should be conserved when all the spin directions are reversed. If this were the case, $\overline{s_1^{(\gamma)} s_2^{(0)}}$ and $\overline{s_1^{(0)} s_2^{(\gamma)}}$ should be equal to zero. However, it will be shown that due to the exchange interaction, even a small external field of 10–100 mT breaks the time-reversal symmetry and leads to spin polarization in nonequilibrium conditions. To show this, the kinetic equations for $\overline{s_1^{(\gamma)} s_2^{(0)}}$, $\overline{s_1^{(0)} s_2^{(\gamma)}}$ and the spin polarizations $\overline{s_1^{(\alpha)}}$, $\overline{s_1^{(\alpha)}}$ should be given.

I start from the expressions for spin polarizations in the electron-hole mechanism

$$\begin{aligned} \frac{d}{dt} \overline{s_1^{(\alpha)}} &= -\frac{E_{ex}}{\hbar} \epsilon_{\alpha\beta\gamma} \overline{s_1^{(\beta)} s_2^{(\gamma)}} + \epsilon_{\alpha\beta\gamma} \Omega_1^{(\beta)} \overline{s_1^{(\gamma)}} - W_1^{(\text{out})} \overline{s_1^{(\alpha)}} \\ &- \gamma_t \overline{s_1^{(\alpha)} s_2^{(0)}} + \gamma_s (\overline{s_1^{(0)} s_2^{(\alpha)}} - \overline{s_1^{(\alpha)} s_2^{(0)}}), \end{aligned} \quad (20)$$

$$\begin{aligned} \frac{d}{dt} \overline{s_2^{(\alpha)}} &= \frac{E_{ex}}{\hbar} \epsilon_{\alpha\beta\gamma} \overline{s_1^{(\beta)} s_2^{(\gamma)}} + \epsilon_{\alpha\beta\gamma} \Omega_2^{(\beta)} \overline{s_2^{(\gamma)}} - W_2^{(\text{out})} \overline{s_2^{(\alpha)}} \\ &- \gamma_t \overline{s_1^{(0)} s_2^{(\alpha)}} + \gamma_s (\overline{s_1^{(\alpha)} s_2^{(0)}} - \overline{s_1^{(0)} s_2^{(\alpha)}}). \end{aligned} \quad (21)$$

The first term on the right-hand side of Eqs. (20) and (21) describes the mutual precession of spins with frequency E_{ex}/\hbar . The second term stands for the spin precession in local fields. The third one shows that the spin polarization is lost when the electron or hole leaves the critical pair. The electron and hole spins can also be lost due to the formation of a spin-polarized triplet exciton with the rate γ_t . Note that the recombination of the spin on site 1 requires a hole on site 2 and therefore the relaxation of spin on site 1 is proportional to $\overline{s_1^{(\alpha)} s_2^{(0)}}$. The singlet exciton formation cannot relax the total spin but leads to redistribution of spin polarization between the sites with the rate γ_s .

When the bipolaron mechanism is considered, $1 \rightarrow 2$ hop is an analog of the singlet exciton formation, and γ_s should be substituted with $W_{21}/2$. There is no analog of triplet exciton formation in the bipolaron mechanism, and γ_t should be substituted with zero in Eqs. (20) and (21). Also $W_2^{(\text{out})}$ should

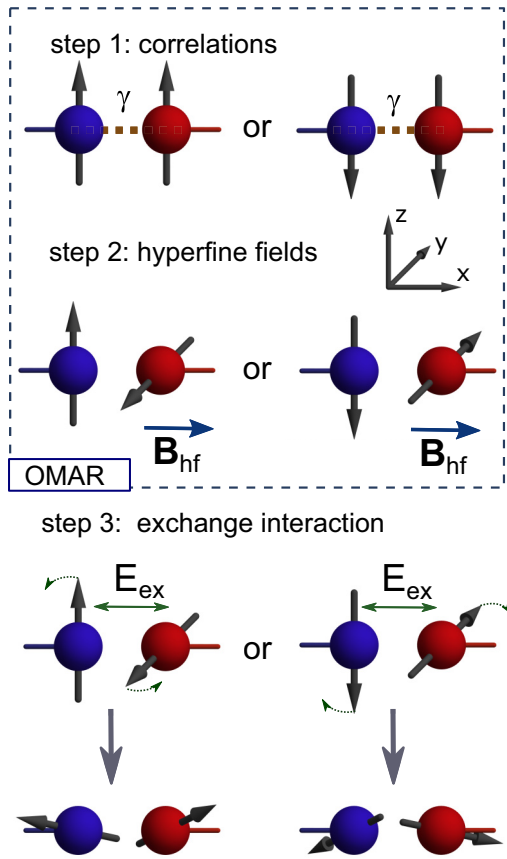


FIG. 3. The three steps that lead to spin polarization of electrons and holes on the trapping sites. In the first step, the spins become correlated due to the different rates of singlet and triplet exciton formation. In the second step, the correlations are modified due to spin precession in effective on-site fields. It is shown with 90° rotation of the hole spin around the x axis. The modified correlations correspond to the coherent combination of singlet and triplet states. In the third step, the spin polarization precesses around the direction of the total spin. Initial rotation directions and the spin directions after 90° rotation are shown. Spin polarization along the x axis of both electron and hole (averaged over the left and right sides of the picture) appears.

be substituted with $W_2^{(in)}$ in Eq. (21) because the B-type site cannot lose its last electron but loses its spin polarization when it becomes double occupied.

Note that the exchange interaction leads to spin polarization only when $\overline{s_1^{(\alpha)} s_2^{(\beta)}} - \overline{s_1^{(\beta)} s_2^{(\alpha)}} \neq 0$. Such correlations correspond to the coherent combination of singlet and triplet states of the electron-hole pair. Therefore the overall picture of dynamic spin polarizations can be described with the three steps that are shown in Fig. 3. In the first step, the probabilities of singlet and triplet states of the polaron pair are no longer in equilibrium due to the different rates of singlet and triplet exciton formation or due to the current and double occupation possibility. This means that spins of the carriers become correlated. In Fig. 3 this is schematically shown with both the spins directed either up or down. It is important that electron and hole spin polarizations averaged over the left and right sides of the figure are zero.

In the second step, the spin precession with different frequencies Ω_1 and Ω_2 leads to a coherent combination of singlet and triplet states and to the correlations with $\overline{s_1^{(\alpha)} s_2^{(\beta)}} - \overline{s_1^{(\beta)} s_2^{(\alpha)}} \neq 0$. In Fig. 3 this is schematically shown with 90° rotation of hole spin on site 2 around the x axis. These two steps are common for the theory of OMAR.

In the third step, exchange interaction leads to mutual precession of spins, or, which is the same, to precession of spins s_1 and s_2 around the direction of $s_1 + s_2$. In Fig. 3 the initial direction of this precession is shown together with the result of such a precession over angle $\pi/2$. The electron has negative polarization in the x direction both on the left and on the right side of the figure. This means that averaged electron spin polarization appears.

At this point the polarizations of electron and hole are opposite because the first terms on the right-hand side of Eqs. (20) and (21) have equal absolute values and different signs. However, other terms on the right-hand side of Eqs. (20) and (21) are different, and the precession of spins with different frequencies Ω_1 and Ω_2 and different rates of electron and hole spin relaxation lead to nonzero averaged spin $\overline{s_1} + \overline{s_2}$. It appears that usually after the averaging over hyperfine fields the spin polarizations on sites 1 and 2 have the same direction.

The kinetic equations for $\overline{s_1^{(\alpha)} s_2^{(0)}}$ and $\overline{s_1^{(0)} s_2^{(\alpha)}}$ are similar to the equations for $\overline{s_1^{(\alpha)}}$ and $\overline{s_1^{(0)}}$. However, the terms describing the transitions of electrons and holes between the bottleneck and other parts of the percolation cluster are different,

$$\begin{aligned} \frac{d}{dt} \overline{s_1^{(\alpha)} s_2^{(0)}} &= -\frac{E_{ex}}{\hbar} \epsilon_{\alpha\beta\gamma} \overline{s_1^{(\beta)} s_2^{(\gamma)}} + \epsilon_{\alpha\beta\gamma} \Omega_1^{(\beta)} \overline{s_1^{(\gamma)} s_2^{(0)}} \\ &\quad - (W_1^{(out)} + W_2^{(out)} + W_2^{(in)} + \gamma_t) \overline{s_1^{(\alpha)} s_2^{(0)}} \\ &\quad + W_2^{(in)} \overline{s_1^{(\alpha)}} + \gamma_s (\overline{s_1^{(0)} s_2^{(\alpha)}} - \overline{s_1^{(\alpha)} s_2^{(0)}}), \end{aligned} \quad (22)$$

$$\begin{aligned} \frac{d}{dt} \overline{s_1^{(0)} s_2^{(\alpha)}} &= \frac{E_{ex}}{\hbar} \epsilon_{\alpha\beta\gamma} \overline{s_1^{(\beta)} s_2^{(\gamma)}} + \epsilon_{\alpha\beta\gamma} \Omega_2^{(\beta)} \overline{s_1^{(0)} s_2^{(\gamma)}} \\ &\quad - (W_2^{(out)} + W_1^{(in)} + W_1^{(out)} + \gamma_t) \overline{s_1^{(0)} s_2^{(\alpha)}} \\ &\quad + W_1^{(in)} \overline{s_2^{(\alpha)}} + \gamma_s (\overline{s_1^{(\alpha)} s_2^{(0)}} - \overline{s_1^{(0)} s_2^{(\alpha)}}). \end{aligned} \quad (23)$$

To consider the bipolaron mechanism, one should substitute γ_s with $W_{21}/2$, substitute γ_t with zero, and mutually exchange $W_2^{(in)}$ and $W_2^{(out)}$.

Equations (9)–(23) compose a system of 21 linear equations that should be solved under stationary conditions together with Eqs. (1)–(5), which describe electric current and exciton generation. However, in any case all the spin correlations and polarizations are proportional to G . Therefore it is possible to express $\sum_{\alpha} \overline{s_1^{(\alpha)} s_2^{(\alpha)}} = \mathcal{T}_s G$, where \mathcal{T}_s has the dimensionality of time. This allows one to use Eqs. (3) and (6).

In the electron-hole mechanism the rate G of generation of spin correlation can be expressed in terms of \mathcal{T}_s as follows:

$$G = \frac{1}{16} \frac{(\gamma_s - \gamma_t) \overline{n_1 n_2}}{1 + \mathcal{T}_s (\gamma_s - \gamma_t) / 4}. \quad (24)$$

Its substitution into Eq. (1) leads to Eq. (3) with

$$\gamma_{eh} = \gamma_t + \frac{(\gamma_s - \gamma_t)}{4 + \mathcal{T}_s (\gamma_s - \gamma_t)}. \quad (25)$$

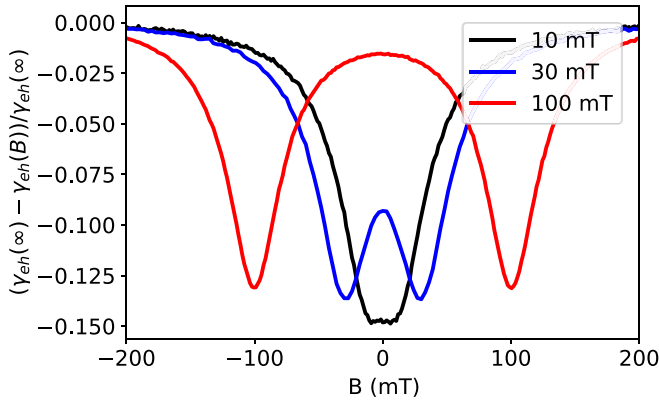


FIG. 4. The shape of $\gamma_{eh}(B)$ dependence with different exchange fields B_{ex} shown in the legend.

In the bipolaron mechanism, similar arguments lead to the expression

$$\kappa_{bp} = \frac{1}{1 + W_{21}T_s/2}. \quad (26)$$

IV. EXCITON FORMATION RATE AND ORGANIC MAGNETORESISTANCE

Exchange interaction modifies the shape of OMAR and the dependence of the exciton formation rate γ_{eh} on applied magnetic field B . This can help to identify situations where dynamic spin polarization occurs in an organic semiconductor. Magnetoresistance and $\gamma_{eh}(B)$ dependence are related in the considered model in the electron-hole mechanism due to Eq. (4). The shape of OMAR in the bipolaron mechanism has similar properties. Therefore only the shape of $\gamma_{eh}(B)$ dependence is considered in this section for definiteness.

The exciton formation rate is calculated with the numeric solution of Eqs. (9)–(23). The typical value of hyperfine field $\Delta_B = 10$ mT is considered. The exchange interaction significantly modifies OMAR when the “exchange field” $B_{ex} = E_{ex}/g\mu_b$ is larger than or comparable to the hyperfine field $B_{ex} \gtrsim \Delta_B$. Therefore values of B_{ex} from 10 to 100 mT are discussed in this section.

In Fig. 4 the calculated dependence $\gamma_{eh}(B)$ is shown. It is compared to the value $\gamma_{eh}(\infty)$ in high magnetic fields where the exciton generation rate is saturated. The singlet and triplet exciton formation rates are considered to be $\gamma_s = 20 \mu\text{s}^{-1}$ and $\gamma_t = 4 \mu\text{s}^{-1}$, respectively. These rates are ~ 10 times slower than the spin precession in the hyperfine field. The transitions of electrons and holes between sites 1 and 2 and the rest of the percolation cluster are described with the rates $W_1^{(in)} = 30 \mu\text{s}^{-1}$, $W_2^{(in)} = 100 \mu\text{s}^{-1}$, $W_1^{(out)} = 5 \mu\text{s}^{-1}$, and $W_2^{(out)} = 1 \mu\text{s}^{-1}$. The relatively small values $W_1^{(out)}$ and $W_2^{(out)}$ show that sites 1 and 2 are efficient traps for an electron and hole, respectively. These parameters were considered to be the same for all the bottlenecks that control the transport. The averaging was made over 10^4 random values of hyperfine fields $\mathbf{B}_{hf}^{(1)}$ and $\mathbf{B}_{hf}^{(2)}$.

The exchange interaction splits the zero-field peak of $\gamma_{eh}(B)$ dependence. This splitting is small when $B_{ex} \lesssim \Delta_B$. This result qualitatively agrees with the calculations made

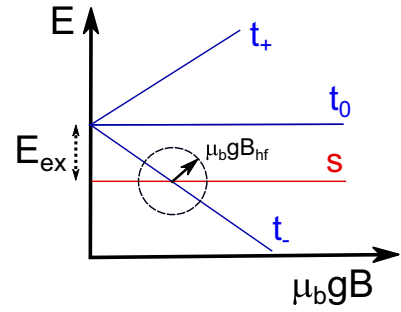


FIG. 5. Energies of the triplet and singlet spin states in a magnetic field. The circle shows where the hyperfine interaction can efficiently mix the states.

in Ref. [23], where it was compared with the magnetoresistance measured in tris(8-hydroxyquinolino)aluminium (Alq_3). When the exchange interaction is strong ($B_{ex} \gtrsim 10\Delta_B$), the $\gamma_{eh}(B)$ shape consists of two peaks at $B = \pm B_{ex}$. This can be explained with the following model (Fig. 5). At zero magnetic field the exchange interaction prevents the hyperfine interaction from mixing singlet and triplet states. In this case the hyperfine interaction does not affect the exciton formation and current. However, the energy of the singlet state E_s does not depend on the magnetic field, while the energy of one of the triplet states E_{t-} decreases with B . When $|B - B_{ex}| \lesssim \Delta_{hf}$, the singlet-triplet mixing due to the hyperfine field becomes efficient. This leads to the peak in $\gamma_{eh}(B)$ dependence.

To the best of the author’s knowledge, such a resonance OMAR shape has never been observed in organic semiconductors. However, similar resonances in magnetoresistance were predicted for spin-polarized scanning tunneling microscopy with a single nonmagnetic dopant [40].

The resonances are sharp in Fig. 5 because the exchange interaction was described with a single phenomenological constant E_{ex} . In principle the exchange interaction can be calculated in organic semiconductors with *ab initio* simulation [41]. It is important, however, that it depends on the overlap integrals between molecules that have an exponentially broad distribution [31]. Therefore one can expect a broad distribution of exchange energies. In real materials it should be determined with numeric simulation. Here, I consider only a simplified model that shows that exchange energy E_{ex} in the bottleneck can vary in order of magnitude

$$B_{ex} = B_{ex}^{(0)} \exp(-\xi), \quad (27a)$$

$$\mathcal{F}_\xi(\xi) = \frac{1}{\xi_{\max}}, \quad \xi \in (0, \xi_{\max}). \quad (27b)$$

The exchange field is always smaller than $B_{ex}^{(0)}$. The value ξ describes its suppression due to the small overlap integral between sites 1 and 2. The distribution density \mathcal{F}_ξ of the suppression factor is flat between zero and ξ_{\max} , which is the maximum suppression that still allows efficient exciton generation. The shapes of $\gamma_{eh}(B)$ dependence for $B_{ex}^{(0)} = 1$ T and $\xi_{\max} = 4$ and 8 are shown in Fig. 6. The splitting of the peak is controlled by the smallest possible exchange energies. When $B_{ex}^{(0)} \exp(-\xi_{\max})$ is large compared with Δ_B , the

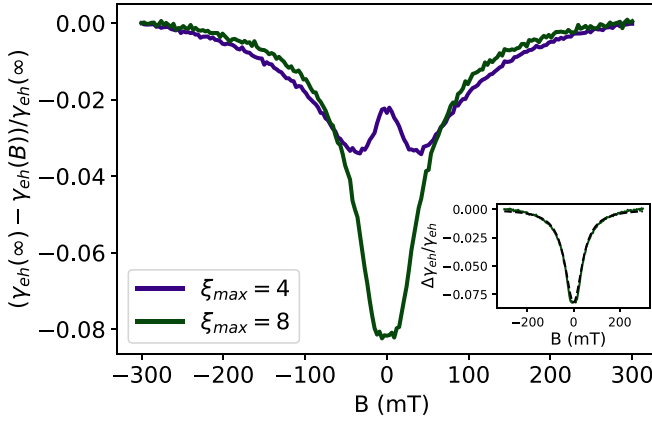


FIG. 6. $\gamma_{eh}(B)$ dependence with the distribution of exchange fields described by Eqs. (27a) and (27b) with different ξ_{\max} described in the legend. The inset shows the comparison between the results for $\xi_{\max} = 8$ (green curve) and Lorentz function $\gamma_{eh}(\infty) - \gamma_{eh}(B) \propto B^2/(B^2 + B_0^2)$ with $B_0 = 45$ mT (black dashed curve).

splitting is clearly observable, while for $B_{ex}^{(0)} \exp(-\xi_{\max}) < \Delta_B$ it is suppressed and the $\gamma_{eh}(B)$ dependence has a Lorentzian shape.

V. DYNAMIC SPIN POLARIZATION

In the presence of exchange interaction the nonequilibrium phenomena that lead to OMAR also yield the spin polarizations of electrons and holes in the bottleneck. This can be understood from the nonzero values of $d\bar{s}_1^{(\alpha)}/dt$ and $d\bar{s}_2^{(\alpha)}/dt$ in Eqs. (20) and (21). The relative polarizations on sites 1 and 2 are defined as P_1 and P_2 , respectively.

$$P_1 = \frac{2\bar{s}_1^{(z)}}{\bar{s}_1^{(0)}}, \quad P_2 = \frac{2\bar{s}_2^{(z)}}{\bar{s}_2^{(0)}}. \quad (28)$$

The polarizations are normalized to the single-occupation probabilities of sites 1 and 2. The averaged polarization is always directed along the axis of the applied magnetic field.

In the electron-hole mechanism of OMAR the produced triplet excitons are also spin polarized, and their polarization is

$$P_{ex} = \frac{\overline{s_1^{(z)} s_2^{(0)}} + \overline{s_1^{(0)} s_2^{(z)}}}{\bar{n}_1 \bar{n}_2}. \quad (29)$$

In both of the OMAR mechanisms, spin current appears. It is different for the two parts of the percolation cluster connected to sites 1 and 2 because the spin is not conserved in the bottleneck. I assume that the electrons that come from the percolation cluster to the bottleneck are not spin polarized. This leads to the following expressions for spin currents $J_s^{(1)}$ and $J_s^{(2)}$ in the bipolaron mechanism:

$$J_s^{(1)} = W_1^{(out)} \bar{s}_1^{(z)}, \quad J_s^{(2)} = -W_2^{(in)} \bar{s}_2^{(z)}. \quad (30)$$

Similar expressions for the spin currents in the electron-hole mechanism are

$$J_s^{(1)} = W_1^{(out)} \bar{s}_1^{(z)}, \quad J_s^{(2)} = -W_2^{(out)} \bar{s}_2^{(z)}. \quad (31)$$

Because the spin currents are directly related to spin polarizations, I discuss only P_1 , P_2 , and P_{ex} . In this section the

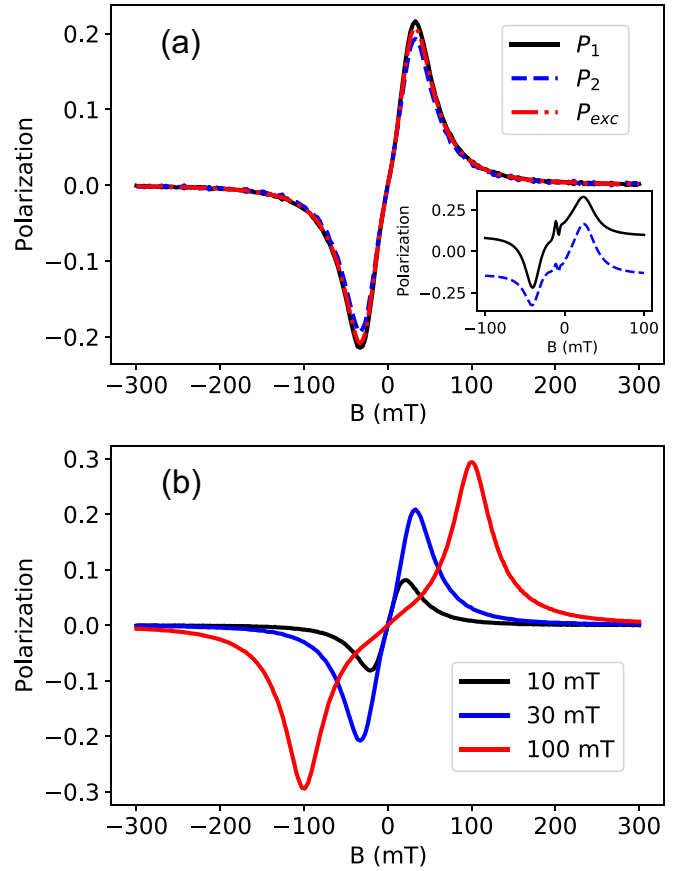


FIG. 7. Dynamic spin polarization calculated numerically and averaged over 10^4 hyperfine fields. (a) The spin polarization of electrons on site 1, holes on site 2, and triplet excitons for the exchange field $B_{ex} = 30$ mT. The inset shows the typical spin polarizations without averaging over hyperfine fields. (b) The triplet exciton spin polarization at different exchange fields shown in the legend.

spin polarizations are calculated numerically under stationary conditions for the systems described in Sec. IV. In Fig. 7(a) the magnetic field dependence of P_1 , P_2 , and P_{ex} is shown for the exchange field $B_{ex} = 30$ mT and the other conditions corresponding to Fig. 4. The polarizations almost coincide in this situation. Some details about their coincidence are given in Sec. VI. Note that although the signs of $d\bar{s}_1^{(\alpha)}/dt$ and $d\bar{s}_2^{(\alpha)}/dt$ in Eqs. (20) and (21) are different when spin polarizations are zero, the resulting polarizations that take into account the spin transfer between molecules and (most importantly) the averaging over the hyperfine fields have the same sign. The inset in Fig. 7(a) shows the typical spin polarizations P_1 and P_2 without the averaging over hyperfine fields. They have the same sign when B is close to $\pm B_{ex}$ and different signs otherwise.

Figure 7(b) shows the triplet exciton polarization at different exchange fields. The shape of the dependence $P_{ex}(B)$ is almost independent of B_{ex} when $B_{ex} \leq \Delta_{hf}$, while its amplitude grows with B_{ex} . For large exchange energy the shape of the dependence contains the two peaks at $B = \pm B_{ex}$ in agreement with Fig. 5.

The results for the broad distribution of exchange energies described with Eqs. (27a) and (27b) are shown in Fig. 8.

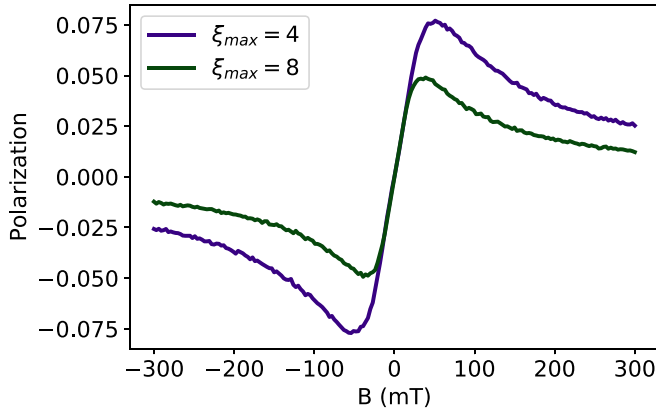


FIG. 8. Dynamic polarization with the broad distribution of exchange fields described by Eqs. (27a) and (27b) with ξ_{\max} shown in the legend.

Similarly to the $\gamma_{eh}(B)$ dependence shown in Fig. 6, the peaks in the dependence of polarization on the applied field are smeared due to the distribution of the exchange energies. However, even when the splitting of the zero-field peak in $\gamma_{eh}(B)$ dependence is hardly observable (as it is in the case of $\xi_{\max} = 8$), the spin polarization is not completely suppressed. The splitting of the zero-field peak depends on the minimal possible exchange energy, while the spin polarization in magnetic field B depends on the probability for the exchange field B_{ex} to be comparable to B .

VI. SPIN POLARIZATION IN RESONANCE

The results of numeric simulation provided in Sec. V show that spin polarization is the strongest in the “resonance situation” when $B = B_{ex} \gg B_{hf}$. This situation is studied in detail in this section. The electron-hole mechanism of OMAR is considered for definiteness.

To further simplify the theory, I assume that the singlet exciton formation rate is fast ($\gamma_s \gg W_1^{(in)} + W_1^{(out)} + W_2^{(in)} + W_2^{(out)}$) and the triplet exciton formation rate is very slow ($\gamma_t \ll W_1^{(out)} + W_2^{(out)}$). The spin precession in the hyperfine field is fast compared with hops and exciton formation rates ($\mu_b g B_{hf} \gg \hbar \gamma_s$).

The singlet electron-hole pair forms an exciton almost immediately after it appears. The electron-hole pair in the state t_- can easily change its state to singlet and also form a singlet exciton. However, the pairs in states t_+ and t_0 usually dissociate due to the electron and hole leaving sites 1 and 2. Sometimes, however, such a pair forms a triplet exciton due to the finite rate γ_t . Even at this point it is clear that the triplet excitons are strongly spin polarized because no t_- triplet excitons appear.

These assumptions allow one to reduce the system (9)–(23) for 21 “spin variables” and the joint equations for “charge” variables \bar{n}_1 , \bar{n}_2 , and $\bar{n}_1 \bar{n}_2$ to a system of six linear equations. The new equations describe the system in terms of the following variables. p_+ and p_0 are the probabilities for the bottleneck to be occupied by the electron-hole pair in t_+ and t_0 states, respectively. The probabilities of the bottleneck to be occupied by electrons and holes in singlet or t_- states are

neglected due to the fast singlet exciton generation rate and efficient coupling between the singlet state and the t_- state. p_1 and p_2 are the probabilities for the occupation of sites 1 and 2, respectively, while the second site is unoccupied. p_{1s} is the difference between the probabilities for site 1 to be occupied by a spin-up and a spin-down electron while site 2 is empty. p_{2s} is a similar quantity for site 2.

Polarizations P_1 , P_2 , and P_{ex} are expressed in these notations as follows:

$$P_{ex} = \frac{p_+}{p_+ + p_0}, \quad (32a)$$

$$P_1 = \frac{p_+ + p_{1s}}{p_+ + p_0 + p_1}, \quad P_2 = \frac{p_+ + p_{2s}}{p_+ + p_0 + p_2}. \quad (32b)$$

Equations (32a) and (32b) show that triplet exciton polarization is related only to the states when both sites of the bottleneck are occupied, while the polarizations P_1 and P_2 are also affected by states when only one of the sites is occupied.

The system of equations for p_ζ , where $\zeta = +, 0, 1, 2, 1s, 2s$, follows from the stationary conditions $dp_\zeta/dt = 0$. The stationary conditions for p_+ yield

$$\frac{p_1 + p_{1s}}{4} W_2^{(in)} + \frac{p_2 + p_{2s}}{4} W_1^{(in)} = (W_1^{(out)} + W_2^{(out)}) p_+. \quad (33)$$

The electron-hole pair in the t_+ state can appear when an electron or hole is trapped on the corresponding site of the bottleneck while the second site is occupied. When the occupied site is not spin polarized (for example, when $p_1 = 1$, $p_{1s} = 0$ and the hole becomes trapped on site 2), any of the four spin states of the electron-hole pair appears with equal probability. When the site is fully spin polarized ($p_1 = p_{1s} = 1$), the probability of a t_+ state after the hole trapping is 1/2. The electron-hole pair dissociates when the electron or hole leaves the bottleneck. The probability of triplet exciton formation γ_t is neglected in comparison to $W_1^{(out)} + W_2^{(out)}$.

The probability of appearance of the t_0 state is not affected by spin polarization of trapping sites leading to the stationary condition for p_0

$$\frac{p_1}{4} W_2^{(in)} + \frac{p_2}{4} W_1^{(in)} = (W_1^{(out)} + W_2^{(out)}) p_0. \quad (34)$$

The stationary conditions for the probabilities p_1 and p_2 lead to the equations

$$W_2^{(out)}(p_+ + p_0) + W_1^{(in)}(1 - p_1 - p_2 - p_+ - p_0) = (W_1^{(out)} + W_2^{(in)}) p_1, \quad (35a)$$

$$W_1^{(out)}(p_+ + p_0) + W_2^{(in)}(1 - p_1 - p_2 - p_+ - p_0) = (W_2^{(out)} + W_1^{(in)}) p_2. \quad (35b)$$

The stationary conditions for p_{1s} and p_{2s} read

$$W_2^{(out)} p_+ = (W_1^{(out)} + W_2^{(in)}) p_{1s}, \quad (36a)$$

$$W_1^{(out)} p_+ = (W_2^{(out)} + W_1^{(in)}) p_{2s}. \quad (36b)$$

The system of equations (33), (34), (35a), (35b), (36a), and (36b) can be solved analytically, but the solution is quite cumbersome. Here, it is given for the specific “symmetrical” case $W_1^{(in)} = W_2^{(in)} = W^{(in)}$, $W_1^{(out)} = W_2^{(out)} = W^{(out)}$. In this

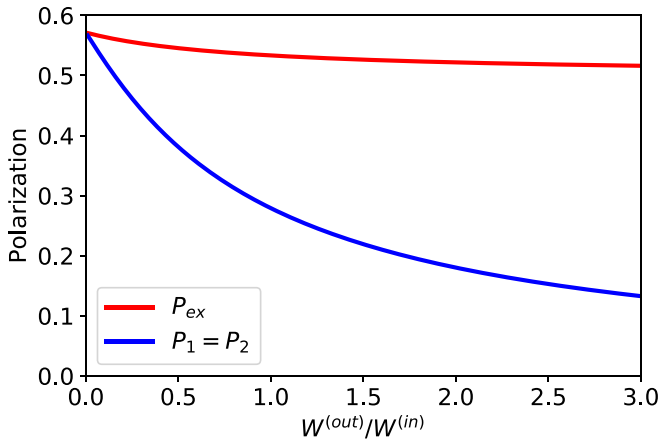


FIG. 9. Exciton spin polarization P_{ex} and electron or hole spin polarization $P_1 = P_2$ under the resonance conditions.

case, $p_1 = p_2$ and $p_{1s} = p_{s2}$. All p_ζ are functions of the ratio $w = W^{(out)}/W^{(in)}$.

The spin polarization p_{1s} of site 1 is related to the triplet occupation number p_+ as follows:

$$p_{1s} = \frac{wp_+}{w+1}. \quad (37)$$

The triplet occupation probabilities are proportional to the probability p_1 of the occupation of a single site.

$$p_0 = \frac{p_1}{4w}, \quad p_+ = \frac{p_1}{4w} \frac{1+w}{3/4+w}. \quad (38)$$

The analytical expression for p_1 is

$$p_1 = \frac{4w(4w+3)}{16w^3 + 52w^2 + 37w + 7}. \quad (39)$$

The spin polarizations P_1 , P_2 , and P_{ex} then should be calculated from Eqs. (32a) and (32b). The result of such a calculation is shown in Fig. 9. When $W^{(in)} \gg W^{(out)}$, the polarizations $P_1 = P_2$ and P_{ex} coincide. Both of the trapping sites are almost always occupied, and p_1 can be neglected in comparison to p_0 and p_+ . p_+ is equal to $4p_0/3$ in this case leading to $P_{ex} = P_1 = P_2 = 4/7$. This is the largest spin polarization possible in the discussed model. Note that in Sec. V, $W_1^{(in)} \gg W_2^{(out)}$ and $W_2^{(in)} \gg W_2^{(out)}$ were considered. Figure 7 shows that polarizations P_1 , P_2 , and P_{ex} coincide in this case even for the nonresonance situation.

In the opposite limit $W^{(out)} \gg W^{(in)}$ the probabilities of the t_+ and t_0 states are equal leading to $P_{ex} = 1/2$. Polarizations P_1 and P_2 are small in this limit.

VII. DISCUSSION

Dynamic spin polarization was observed in nonorganic GaAs quantum dots due to the circular polarization of photoluminescence. It was possible due to the strong spin-orbit interaction in GaAs that allows radiative recombination of excitons with angular momentum equal to unity. In organic semiconductors such a detection is not an easy task because usually only singlet excitons recombine radiatively. The radiative recombination of triplets in organics is called phosphorescence and can be achieved by the introduction of

certain impurities (the so-called phosphors) to organic semiconductors. It makes the optical detection of dynamic spin polarization in organics possible at least in theory. However, such a detection is related to additional restrictions that are out of the scope of the provided model: The spin of a triplet exciton should be conserved during the transition to such a phosphor and the following recombination process.

However, organic semiconductors also have advantages over quantum dots when dynamic spin polarization is considered. Spin-phonon interaction in nonorganic semiconductors leads to fast spin relaxation that suppresses circular polarization of luminescence in quantum dots at temperatures $T \gtrsim 10$ K [24]. However, OMAR and a strong spin-valve effect exist both at low and room temperatures due to the weak spin-orbit interaction in organic materials. This makes it possible for dynamic spin polarization to also exist at room temperature.

The long spin diffusion length measured in some organic semiconductors gives hope that the spin polarization can be detected in transport measurements in hybrid devices with ferromagnetic contacts. Another possibility is the muon spin rotation experiments that were able to detect spin polarization in working spin-valve devices. Actually, the author believes that it may be relevant to revisit organic spin-valve experiments in view of the results of this paper. Usually, only two possibilities were considered for an organic spin valve: The spin is injected from the first ferromagnetic contact and is detected by the second one, or the spin valve is due to the tunneling through pinholes in the organic layer. Now a third assumption should be added: The spin can be generated inside the organic layer. The external fields of ~ 100 mT required for such a generation can be related, for example, to fringe fields of magnetic contacts [42].

A significant dynamic spin polarization requires the energies of exchange between electrons and holes on different molecules in the bottleneck to be larger than or comparable to the energy of hyperfine interaction of electron and nuclear spins. The existing estimates of the exchange energies are quite controversial. In Ref. [23] the value $B_{ex} = 0.2$ mT was extracted from the comparison of measured OMAR shape with theory. Such a value is clearly insufficient for the significant spin polarization. However, such an estimate of the exchange energy can be complicated if B_{ex} has broad distribution, as follows from Fig. 6. The exchange interaction between electrons localized on different molecules was also invoked in Ref. [14] to describe the absence of the Hanle effect in organic spin valves. Exchange energies corresponding to $B_{ex} \gtrsim 0.1$ T were considered to be possible. Perhaps the typical exchange energies in an organic semiconductor can be very different in different samples and depend not only on chemical structure but also on the concentration of injected charge carriers. Strong dynamic spin polarization can occur in samples where the condition $B \sim B_{ex} \gtrsim B_{hf}$ is satisfied.

In this paper the minimal model for dynamical spin polarization is considered. Several generalizations of this model may be relevant for some organic materials. For example, the difference in the electron and hole g factor can significantly modify the magnetoresistance shape [43]. The exchange energies and intermolecular hopping rates can be correlated, which was not considered. In the applied model the electrons

and holes that come to the bottleneck from the percolation cluster are presumed not to be spin polarized. However, if the electron and hole spin relaxation is not very efficient, the spin accumulation will result in the initial spin polarization of electrons and holes trapped at the bottleneck. This may increase spin polarization and make it larger than 4/7, which is the limiting value of the considered model.

The description of hyperfine interaction was made with the static “hyperfine fields.” This stands for the theoretical limit of a large number N_n of nuclear spins interacting with a single electron spin. In particular, in real materials with finite N_n the momentum conservation law should lead to the polarization of nuclear spins when electron and hole spins become polarized. However, the averaged polarization of nuclear spins is proportional to $1/N_n$. Also the polarization of nuclear spins in a molecule occurs only when its HOMO or LUMO is occupied by an electron or hole, respectively. The concentrations of electrons and holes are small in many organic semiconductors. This allows one to presume that even slow nuclear spin relaxation can effectively depolarize the nuclei and consider the direction of hyperfine fields to be random.

In materials with small N_n and relatively large electron and hole concentrations the nuclear spin relaxation can be inefficient, and nuclear spin polarization may occur. In this case it can be detected in nuclear magnetic resonance measurements.

In conclusion, it was shown that exchange interaction between electrons and holes localized on different molecules leads to spin polarization in organic semiconductors where OMAR is observed. For the polarization to be significant the exchange interaction should be comparable to or larger than hyperfine interaction of electron and nuclear spins. The exchange interaction also modifies the shape of OMAR. However, such a modification can be masked by a broad distribution of exchange energies. This broad distribution does not completely suppress the spin polarization.

ACKNOWLEDGMENTS

The author is grateful to D. S. Smirnov, V. V. Kabanov, V. I. Dediu, and Y. M. Beltukov for many fruitful discussions. The support from the Foundation for the Advancement of Theoretical Physics and Mathematics “Basis” is greatly acknowledged.

APPENDIX: MAGNETORESISTANCE IN THE ELECTRON-HOLE MECHANISM

To calculate the magnetoresistance in the electron-hole mechanism, the current should be expressed as the rate of

trapping on sites 1 and 2

$$J = e(1 - \bar{n}_1)W_1^{(in)} - eW_1^{(out)}\bar{n}_1, \quad (\text{A1})$$

$$J = e(1 - \bar{n}_2)W_2^{(in)} - eW_2^{(out)}\bar{n}_2. \quad (\text{A2})$$

Equation (A1) shows that the electron cannot be trapped on site 1 if it is already occupied and that all the electrons that are trapped and do not leave site 1 contribute to exciton generation and current. Equation (A2) is a similar expression for site 2.

The current given by Eqs. (A1) and (A2) is equal to the current given by (3). This system of equations should be complemented by the master equation for joined occupation probability $\bar{n}_1\bar{n}_2$

$$\frac{d}{dt}\bar{n}_1\bar{n}_2 = 0 = W_1^{(in)}\bar{n}_2 + W_2^{(in)}\bar{n}_1 - [\tilde{W}_{12} + \gamma_{eh}(B)]\bar{n}_1\bar{n}_2. \quad (\text{A3})$$

Here, $\tilde{W}_{12} = W_1^{(in)} + W_1^{(out)} + W_2^{(in)} + W_2^{(out)}$.

The solution of Eqs. (3) and (A1)–(A3) yields the following expressions for n_1 and n_2 :

$$\bar{n}_1 = \frac{W_1^{(in)} - \tilde{\gamma}\bar{n}_1\bar{n}_2}{W_1^C}, \quad (\text{A4})$$

$$\bar{n}_2 = \frac{W_2^{(in)} - \tilde{\gamma}\bar{n}_1\bar{n}_2}{W_2^C}. \quad (\text{A5})$$

Here, $W_1^C = W_1^{(in)} + W_1^{(out)}$, and $W_2^C = W_2^{(in)} + W_2^{(out)}$.

The current J and joined occupation probability $\bar{n}_1\bar{n}_2$ are expressed as follows:

$$J = \frac{e\gamma_{eh}W_1^{(in)}W_2^{(in)}\tilde{W}_{12}}{W_1^CW_2^C\tilde{W}_{12} + \gamma_{eh}\mathcal{W}}, \quad (\text{A6})$$

$$\bar{n}_1\bar{n}_2 = \frac{W_1^{(in)}W_2^{(in)}\tilde{W}_{12}}{W_1^CW_2^C\tilde{W}_{12} + \gamma_{eh}\mathcal{W}}. \quad (\text{A7})$$

Here, $\mathcal{W} = W_1^CW_2^C + W_1^CW_1^{(in)} + W_2^CW_2^{(in)}$.

The magnetoresistance can be expressed as $(J(0) - J(B))/J(B)$. When the effect of spin correlations on conductivity is small, the magnetoresistance is also small [$|J(0) - J(B)| \ll J(0)$], and Eq. (4) can be derived from Eq. (A6) with C_{eh} equal to

$$C_{eh} = \frac{W_1^CW_2^C\tilde{W}_{12}}{W_1^CW_2^C\tilde{W}_{12} + \gamma_{eh}(0)\mathcal{W}}. \quad (\text{A8})$$

Here, $\gamma_{eh}(0)$ is calculated in zero magnetic field.

- [1] S. Forrest, The path to ubiquitous and low-cost organic electronic appliances on plastic, *Nature (London)* **428**, 911 (2004).
- [2] Q. Wei, N. Fei, A. Islam, T. Lei, L. Hong, R. Peng, X. Fan, L. Chen, P. Gao, and Z. Ge, Small-molecule emitters with high quantum efficiency: Mechanisms, structures, and applications in OLED devices, *Adv. Opt. Mater.* **6**, 1800512 (2018).
- [3] C. J. Brabec, N. S. Sariciftci, and J. C. Hummelen, Plastic solar cells, *Adv. Opt. Mater.* **11**, 15 (2001).

- [4] R. Zhou, Z. Jiang, C. Yang, J. Yu, J. Feng, M. A. Adil, D. Deng, W. Zou, J. Zhang, K. Lu, W. Ma, F. Gao, and Z. Wei, All-small-molecule organic solar cells with over 14 efficiency by optimizing hierarchical morphologies, *Nat. Commun.* **10**, 5393 (2019).
- [5] B. Qiu, Z. Chen, S. Qin, J. Yao, W. Huang, L. Meng, H. Zhu, Y. M. Yang, Z.-G. Zhang, and Y. Li, Highly efficient all-small-molecule organic solar cells with appropriate active

- layer morphology by side chain engineering of donor molecules and thermal annealing, *Adv. Mater. (Weinheim)* **32**, 1908373 (2020).
- [6] S. Allard, M. Forster, B. Souharce, H. Thiem, and U. Scherf, *Angew. Chem. Int. Ed.* **47**, 4070 (2008).
- [7] C.-A. Di, F. Zhang, and D. Zhu, Multi-functional integration of organic field-effect transistors (OFETs): Advances and perspectives, *Adv. Mater. (Weinheim)* **25**, 313 (2013).
- [8] Z. H. Xiong, D. Wu, Z. Vally Vardeny, and J. Shi, Giant magnetoresistance in organic spin-valves, *Nature (London)* **427**, 821 (2004).
- [9] S. Pramanik, C.-G. Stefanita, S. Patibandla, S. Bandyopadhyay, K. Garre, N. Harth, and M. Cahay, Observation of extremely long spin relaxation times in an organic nanowire spin valve, *Nat. Nanotechnol.* **2**, 216 (2007).
- [10] A. J. Drew, J. Hoppler, L. Schulz, F. L. Pratt, P. Desai, P. Shakya, T. Kreouzis, W. P. Gillin, A. Suter, N. A. Morley, V. K. Malik, A. Dubroka, K. W. Kim, H. Bouyanfif, F. Bourqui, C. Bernhard, R. Scheuermann, G. J. Nieuwenhuys, T. Prokscha, and E. Morenzoni, Direct measurement of the electronic spin diffusion length in a fully functional organic spin valve by low-energy muon spin rotation, *Nat. Mater.* **8**, 109 (2009).
- [11] V. A. Dediu, L. E. Hueso, I. Bergenti, and C. Taliani, Spin routes in organic semiconductors, *Nat. Mater.* **8**, 707 (2009).
- [12] G. Schmidt, D. Ferrand, L. W. Molenkamp, A. T. Filip, and B. J. van Wees, Fundamental obstacle for electrical spin injection from a ferromagnetic metal into a diffusive semiconductor, *Phys. Rev. B* **62**, R4790 (2000).
- [13] M. Prezioso, A. Riminucci, I. Bergenti, P. Graziosi, D. Brunel, and V. A. Dediu, Electrically programmable magnetoresistance in multifunctional organic-based spin valve devices, *Adv. Mater. (Weinheim)* **23**, 1371 (2011).
- [14] Z. G. Yu, Suppression of the Hanle Effect in Organic Spintronic Devices, *Phys. Rev. Lett.* **111**, 016601 (2013).
- [15] M. Grünewald, R. Göckeritz, N. Homonnay, F. Würthner, L. W. Molenkamp, and G. Schmidt, Vertical organic spin valves in perpendicular magnetic fields, *Phys. Rev. B* **88**, 085319 (2013).
- [16] J. Kalinowski, M. Cocchi, D. Virgili, P. Di Marco, and V. Fattori, Magnetic field effects on emission and current in Alq₃-based electroluminescent diodes, *Chem. Phys. Lett.* **380**, 710 (2003).
- [17] O. Mermer, G. Veeraraghavan, T. L. Francis, Y. Sheng, D. T. Nguyen, M. Wohlgenannt, A. Köhler, M. K. Al-Suti, and M. S. Khan, Large magnetoresistance in nonmagnetic π -conjugated semiconductor thin film devices, *Phys. Rev. B* **72**, 205202 (2005).
- [18] V. N. Prigodin, J. D. Bergeson, D. M. Lincoln, and A. J. Epstein, Anomalous room temperature magnetoresistance in organic semiconductors, *Synth. Met.* **156**, 757 (2006).
- [19] P. A. Bobbert, T. D. Nguyen, F. W. A. van Oost, B. Koopmans, and M. Wohlgenannt, Bipolaron Mechanism for Organic Magnetoresistance, *Phys. Rev. Lett.* **99**, 216801 (2007).
- [20] W. Wagemans and B. Koopmans, Spin transport and magnetoresistance in organic semiconductors, *Phys. Status Solidi B* **248**, 1029 (2011).
- [21] Z. G. Yu, F. Ding, and H. Wang, Hyperfine interaction and its effects on spin dynamics in organic solids, *Phys. Rev. B* **87**, 205446 (2013).
- [22] T. D. Nguyen, G. Hukic-Markosian, F. Wang, L. Wojcik, X.-G. Li, E. Ehrenfreund, and Z. V. Vardeny, Isotope effect in spin response of π -conjugated polymer films and devices, *Nat. Mater.* **9**, 345 (2010).
- [23] T. D. Nguyen, T. P. Basel, Y.-J. Pu, X.-G. Li, E. Ehrenfreund, and Z. V. Vardeny, Isotope effect in the spin response of aluminum tris(8-hydroxyquinoline) based devices, *Phys. Rev. B* **85**, 245437 (2012).
- [24] D. S. Smirnov, T. S. Shamirzaev, D. R. Yakovlev, and M. Bayer, Dynamic Polarization of Electron Spins Interacting with Nuclei in Semiconductor Nanostructures, *Phys. Rev. Lett.* **125**, 156801 (2020).
- [25] T. S. Shamirzaev, A. V. Shumilin, D. S. Smirnov, J. Rautert, D. R. Yakovlev, and M. Bayer, Dynamic polarization of electron spins in indirect band gap (In,Al)As/AlAs quantum dots in a weak magnetic field: Experiment and theory, *Phys. Rev. B* **104**, 115405 (2021).
- [26] D. S. Smirnov, Dynamic valley polarization in moiré quantum dots, *Phys. Rev. B* **104**, L241401 (2021).
- [27] I. I. Fishchuk, A. Kadashchuk, S. T. Hoffmann, S. Athanasopoulos, J. Genoe, H. Bässler, and A. Köhler, Unified description for hopping transport in organic semiconductors including both energetic disorder and polaronic contributions, *Phys. Rev. B* **88**, 125202 (2013).
- [28] H. Bässler and A. Köhler, Charge transport in organic semiconductors, in *Unimolecular and Supramolecular Electronics I: Chemistry and Physics Meet at Metal-Molecule Interfaces*, edited by R. M. Metzger (Springer, Berlin, 2012), pp. 1–65.
- [29] T. Sueyoshi, H. Fukagawa, M. Ono, S. Kera, and N. Ueno, Low-density band-gap states in pentacene thin films probed with ultrahigh-sensitivity ultraviolet photoelectron spectroscopy, *Appl. Phys. Lett.* **95**, 183303 (2009).
- [30] I. Lange, J. C. Blakesley, J. Frisch, A. Vollmer, N. Koch, and D. Neher, Band Bending in Conjugated Polymer Layers, *Phys. Rev. Lett.* **106**, 216402 (2011).
- [31] A. Massé, P. Friederich, F. Symalla, F. Liu, V. Meded, R. Coehoorn, W. Wenzel, and P. A. Bobbert, Effects of energy correlations and superexchange on charge transport and exciton formation in amorphous molecular semiconductors: An *ab initio* study, *Phys. Rev. B* **95**, 115204 (2017).
- [32] B. I. Shklovskii and A. L. Efros, *Electronic Properties of Doped Semiconductors* (Springer, Berlin, 1984).
- [33] J. Cottaar, L. J. A. Koster, R. Coehoorn, and P. A. Bobbert, Scaling Theory for Percolative Charge Transport in Disordered Molecular Semiconductors, *Phys. Rev. Lett.* **107**, 136601 (2011).
- [34] A. V. Shumilin, V. V. Kabanov, and V. I. Dediu, Magnetoresistance in organic semiconductors: Including pair correlations in the kinetic equations for hopping transport, *Phys. Rev. B* **97**, 094201 (2018).
- [35] A. V. Shumilin and Y. M. Beltukov, System of correlation kinetic equations and the generalized equivalent circuit for hopping transport, *Phys. Rev. B* **100**, 014202 (2019).
- [36] A. V. Shumilin and Y. M. Beltukov, Effect of nonequilibrium correlations on the effective resistances between sites in the theory of hopping conductivity, *Phys. Solid State* **61**, 2090 (2019).
- [37] A. V. Shumilin, Microscopic theory of organic magnetoresistance based on kinetic equations for quantum spin correlations, *Phys. Rev. B* **101**, 134201 (2020).
- [38] S. Hoshino and H. Suzuki, Electroluminescence from triplet excited states of benzophenone, *Appl. Phys. Lett.* **69**, 224 (1996).

- [39] M. A. Baldo, D. F. O'Brien, Y. You, A. Shoustikov, S. Sibley, M. E. Thompson, and S. R. Forrest, Highly efficient phosphorescent emission from organic electroluminescent devices, *Nature (London)* **395**, 151 (1998).
- [40] S. R. McMillan, N. J. Harmon, and M. E. Flatté, Image of Dynamic Local Exchange Interactions in the dc Magnetoresistance of Spin-Polarized Current through a Dopant, *Phys. Rev. Lett.* **125**, 257203 (2020).
- [41] A. Droghetti, Oxygen doping and polaron magnetic coupling in Alq₃ films, *J. Magn. Magn. Mater.* **502**, 166578 (2020).
- [42] F. Wang, F. Macià, M. Wohlgenannt, A. D. Kent, and M. E. Flatté, Magnetic Fringe-Field Control of Electronic Transport in an Organic Film, *Phys. Rev. X* **2**, 021013 (2012).
- [43] F. J. Wang, H. Bässler, and Z. Valy Vardeny, Magnetic Field Effects in π -Conjugated Polymer-Fullerene Blends: Evidence for Multiple Components, *Phys. Rev. Lett.* **101**, 236805 (2008).